Pergamon

Int. J. Heat Mass Transfer. Vol. 40, No. 12, pp. 2869–2877, 1997
© 1997 Elsevier Science Ltd. All rights reserved
Printed in Great Britain
0017–9310/97 $17.00+0.00

PII: S0017–9310(96)00330–4

A similarity solution for the solidification of a multicomponent alloy

V. R. VOLLER

Saint Anthony Falls Laboratory, Department of Civil Engineering, University of Minnesota, Minneapolis, MN 55455, U.S.A.

(*Received* 19 *July* 1996 *and in final form* 13 *September* 1996)

Abstract—A similarity solution for a multicomponent solidification model is introduced. The model includes a complete coupling of solute and temperature fields in the mushy region, a eutectic reaction, macrosegregation, microsegregation and fluid flow. The similarity solution is demonstrated on comparing its results with predictions obtained from a full numerical solution. © 1997 Elsevier Science Ltd.

1. INTRODUCTION

The development of numerical methods for modeling phase change systems is a major research area in heat and mass transfer. In carrying out these developments two validation/verification questions that need to be addressed are:

(1) Is the complete numerical model, governing equations + boundary conditions + numerical solution, a reasonable representation of the physical reality?
(2) Does the numerical solution scheme accurately solve the governing equations?

The first of these questions involves the comparison with experiments, process measurements and to some extent physical intuition. The notion of a reasonable representation reduces to accessing how useful the results of the modeling exercise are in improving the understanding and operation of a given engineering operation. Answering the second validation/verification question is by and large a problem in numerical analysis. A direct way of accessing the accuracy of a given numerical scheme is to compare predictions against "test solutions", i.e. analytical, semi-analytical or approximate solutions of limiting cases of the model. A weakness in this approach is that these limiting models may be far removed from the system of interest. For example, consider a numerical scheme developed for the solution of a multicomponent alloy solidification model. Testing the performance of this scheme against an analytical solution for a pure material [1] will show up any flaws in the proposed scheme, but will be unable to access how well the scheme handles the solute and temperature coupling in the two phase mushy zone [2], a key feature in a multicomponent alloy.

In this paper a semi-analytical similarity solution of a multicomponent alloy is developed. This solution is applicable to solidification models that include:

(1) coupling of the solute and temperature fields;
(2) eutectic reactions;
(3) microsegregation;
(4) macrosegregation; and
(5) fluid flow.

These are features that make it an excellent test solution for proving numerical schemes designed to model general solidification systems.

2. GOVERNING EQUATIONS

The problem investigated here will involve the unidirectional solidification of a binary-eutectic alloy, e.g. aluminum–copper. This solidification is carried out in an insulated, vertical mold with a cooled constant temperature boundary at $z = 0$, Fig. 1. Initially the liquid alloy in the mold has a uniform solute concentration, $C = C_0$ and a uniform temperature, $T_i = T_L + \Delta T_{SH}$ (the equilibrium liquidus temperature + a super heat). The temperature at the cooled boundary is held fixed at a temperature, T_{chill}, below the solidus temperature of the alloy. In addition the mold is considered to be long enough such that the temperature at the upper boundary, $z = Z_{mold}$, remains fixed at the initial temperature T_i. After solidification starts the domain $0 \leqslant z \leqslant Z_{mold}$ consists of three regions: (i) a fully solid region; (ii) a mushy region comprising a mixture of solid crystals and liquid; and (iii) a fully liquid region. As solid forms in the mushy region the solute phase is rejected into the liquid. At the local scale of the crystal structure, the dendritic arm spaces, the reject solute is redistributed by diffusion processes, setting up microscale concentration profiles, microsegregation. At the scale of the process, due to flows induced by solidification shrinkage advection transport processes dominate. As

NOMENCLATURE

a	numerical coefficient
c	specific heat capacity
C	concentration
$\langle C_s \rangle^s$	intrinsic volume average of solute concentration in solid phase
K	thermal conductivity
k	partition coefficient
L	latent heat
m	slope of the liquids line
R	density ratio
T	temperature
T_F	fusion temperature
T_L	liquidus temperature
U	volume flux of interdentritic fluid.

Greek symbols

β	microsegregation parameter
ΔT_{SH}	super heat
ξ	similarity variable
ρ	density
λ	position of liquidus in ξ space
μ	position of eutectic in ξ space
κ	thermal diffusivity
ϕ	volume fraction of solid.

Subscript

chill	chill face
eut	eutectic
l	liquid
liq	liquidus
mold	top of mold
s	solid.

a result, even though the total amount of solute remains constant in the system a solute concentration profile is established across the solid and mushy regions, macrosegregation.

With regard to the system in Fig. 1 the following assumptions are made:

(1) The solid is fixed, i.e. the morphology of the mushy region is columnar dendritic or consolidated equiaxed.
(2) Within a representative elementary volume (REV) of the mushy region (order of 10^{-2} to 10^{-3} m) the temperature is uniform.
(3) Within the liquid fraction of the REV solutal concentrations are uniform.
(4) Thermodynamic equilibrium holds at the solid–liquid interface, i.e. at the solid–liquid interface in the REV the solid and liquid concentrations of each species are related via the expression $C_s = kC_l$ where k is the equilibrium partition coefficient. This means that the temperature and the liquid solute concentrations in an REV lie on the liquidus surface of the phase diagram.
(5) The temperature is rescaled such that the fusion temperature, T_F, is set to zero and the liquidus line is given by

$$C_l = -mT \tag{1}$$

where $-m$ is the constant slope, see the schematic in Fig. 2.
(6) At the macroscopic scale of a solidification process (order of meters) solutal mass diffusion is negligible.
(7) At the microscopic scale, within the REV, finite solute diffusion in the solid is accounted for with a version of the Clyne and Kurz [3] microsegregation model.
(8) Flow is induced by imposing a density difference between the solid and liquid phases. Within each phase constant density values, ρ_s and ρ_l, are taken.

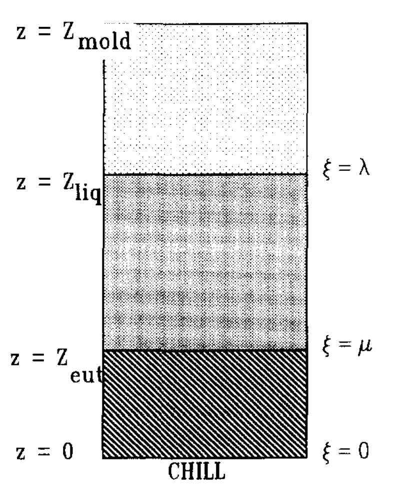

Fig. 1. Test geometry.

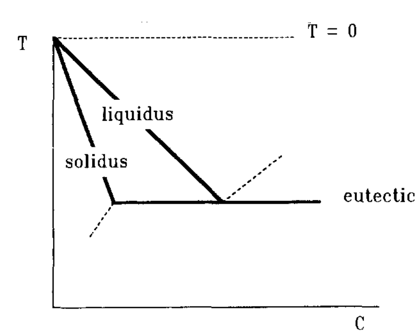

Fig. 2. Schematic of a section of the phase diagram.

(9) A low superheat in the liquid phase is assumed such that heat transfer in the full liquid region can be adequately modeled by heat conduction.
(10) For convenience of presentation, alone, constant values of thermal conductivity, K, specific heat, c, and latent heat, L, have been assumed.

With these assumptions the governing equations, derived from more general multidimensional equations presented in a companion paper [2], are:

In the liquid region $Z_{\text{liq}} \leqslant z$ ($z = Z_{\text{mold}}$ is taken as the far filed condition $z \to \infty$).

Heat

$$\frac{\partial T}{\partial t} = \kappa \frac{\partial^2 T}{\partial z^2} \tag{2}$$

where $\kappa = K/\rho_1 c$ is the liquid thermal diffusivity.

In the mushy region $Z_{\text{eut}} \leqslant z \leqslant Z_{\text{liq}}$.

Heat

$$[(1-\phi)+\phi R]\frac{\partial T}{\partial t} + U\frac{\partial T}{\partial z} = \kappa\frac{\partial^2 T}{\partial z^2} + R\frac{L}{c}\frac{\partial \phi}{\partial t} \tag{3}$$

where ϕ is the volume fraction of solid in an REV, R is the density ratio (ρ_s/ρ_1) and U is the volume flux of inderdendritic liquid.

Concentration

$$[\beta k R\phi + (1-\phi)]\frac{\partial C_1}{\partial t} + U\frac{\partial C_1}{\partial z} = (1-k)RC_1\frac{\partial \phi}{\partial t}. \tag{4}$$

Mass

$$\frac{\partial U}{\partial z} = (1-R)\frac{\partial \phi}{\partial t}. \tag{5}$$

In the solid region $0 \leqslant z \leqslant Z_{\text{eut}}$.

Heat

$$\frac{\partial T}{\partial t} = R\kappa\frac{\partial^2 T}{\partial z^2}. \tag{6}$$

The boundary conditions are

as $z \to \infty$

$$T = T_L + T_{SH}, \quad C_1 = C_0 \tag{7}$$

where C_0 is the initial composition in the liquid phase, $T_L = -mC_0$ is the liquidus temperature corresponding to this composition and ΔT_{SH} is a superheat.

On the moving boundary $z = Z_{\text{liq}}(t)$.

$$T = T_L, \quad \left[\frac{\partial T}{\partial z}\right] = 0, \quad \phi = 0 \tag{8}$$

where the brackets [ ] indicate the discontinuity across the boundary.

On the moving boundary $z = Z_{\text{eut}}(t)$.

$$T = T_{\text{eut}}, \quad \kappa\left[\frac{\partial T}{\partial z}\right] = -R(1-\phi)\frac{dZ_{\text{eut}}}{dt}\frac{L}{c},$$

$$[U] = (1-R)(1-\phi)\frac{dZ_{\text{eut}}}{dt} \tag{9}$$

where the last two terms arise due to the jump in the liquid fraction at the eutectic front.

At $z = 0$

$$T = T_{\text{chill}} < T_{\text{eut}}. \tag{10}$$

In the mushy region, $Z_{\text{eut}} \leqslant z \leqslant Z_{\text{liq}}$, the governing equations are close to those previously presented by Chiareli and Worster [4]. The solute equation, however, is more general. The Chiareli and Worster model assumes complete rejection of the solute as the solid forms ($k = 0$). In the current model k can take finite values between 0 and 1. In addition the current model includes the term, β, not found in the Chiareli and Worster model. This term allows for the modeling of the microsegregation in the solid phase of the REV referred to as "black diffusion". A setting of $\beta = 0$ in equation (4) will model the case of zero solid state diffusion (the Scheil equation), a setting of $\beta = 1$ models the case of complete solid state diffusion (the lever rule). The use of this term in equation (4) also allows for modeling cases of finite back diffusion, $0 < \beta < 1$; a model as noted in a companion paper [2], consistent with the well known Clyne and Kurz [3] microsegregation model.

A major step in the numerical solution of the governing equations is the coupling of the temperature and solute fields through the liquidus line of the phase diagram. Numerical approaches for this coupling can become quite involved [2] and as a result they are difficult to validate. The central objective of the current paper is to develop appropriate semi-analytical solutions for the validation of temperature–solute coupling schemes.

3. A BRIEF REVIEW OF SEMI-ANALYTICAL SOLUTIONS

A semi-analytical solution of a phase change systems involves an analysis, sometimes based on an approximation, that reduces the governing partial differential equations to a set of ordinary differential or algebraic equations. In the context of the example one-dimensional problem introduced above two important classes of semi-analytical solution are outlined below.

3.1. *The heat balance integral (HBI)*

This approach, first proposed by Goodman [5] for Stefan problems, can be used to model one-dimensional phase change that involve no flow or macrosegregation (i.e. equations (4) and (5) are removed from the set of governing equations). In the HBI the temperature profile in the domain is approximated by a series of polynomials (one for each of the solid, mushy and liquid regions) with coefficients chosen to satisfy appropriate boundary conditions. Following the integration of the heat flow equation, equations (2), (3) and (6), the polynomial approximations, typically quadratics, are used to reduce the governing equations to a set of ordinary differential equations in terms of the movement of the solid/mushy and mushy/liquid interface positions. In some cases a similarity solution of the resulting equations can be obtained which reduces the problem to that of solving a set of nonlinear algebraic equations. Tien and Geiger [6] investigate the unidirectional solidification of a binary–eutectic alloy in a semi-infinite domain with a fixed surface temperature at $z = 0$ and in later work [7] with a prescribed varying temperature. Sunderland and co-workers have investigated similar problems in finite domains with fixed surface temperature [8] and convective cooling [9] at $z = 0$. In the work in Refs [6–9] the heat generation term in the mushy region is handled on specifying that the liquid fraction is a function of distance across the mushy region and as such microsegregation is not accurately modeled. This drawback is overcome in the work of Voller [10] who develops a heat balance integral solution of a binary-eutectic alloy solidification based on an enthalpy formulation that allows for treatments of the microsegregation, i.e. the lever rule or Scheil equation.

Using an approach with some similarity to the heat balance integral methods Flemings and Nero [11] developed an approximate solution for the macrosegregation in a binary–eutectic alloy, a phenomena neglected in the heat balance integral models [6–10]. In this approach an analytical expression for the mixture concentration at any point in a semi-infinite casting is obtained on specifying the movement of the solid/mushy and mushy/liquid interfaces and specifying a linear profile for the liquid fraction. Good comparison with experimental measurements of concentration are obtained on matching the prescribed movements of the interfaces to experimental measurements.

3.2. *Similarity solutions*

In a similarity solution a similarity variable, combining the space and time variables, is sought that transforms the governing partial differential equations into a set of ordinary differential equations with the similarity variable as the independent variable. In some cases an analytical solution of the resulting equations can be found, e.g. the Neumann solution of the Stefan problem [1], the Rubinstein solution of plane front alloy solidification [12] and the solution of a mushy phase change with an imposed linear liquid fraction profile [8, 13]. In general, however, a numerical solution of the ordinary differential equations is required; a step which is likely to be far more robust, accurate and less demanding than solving the original governing partial differential equations. In this respect, since no additional physical approximations are made one can have a high degree of confidence that a similarity solution will provide an accurate solution of the given solidification model.

In terms of finding similarity solutions of the unidirectional solidification of binary–eutectic alloys, see Fig. 1, most work has focused on aqueous solutions that exhibit zero solid solubility ($k = 0$), i.e. as the solid forms in the mush there is complete rejection of the solute phase. Braga and Viskanta [14] present a similarity solution for an aqueous solution and compare results with an experiment. In their model the surface temperature at $z = 0$ is fixed at a temperature above the eutectic and fluid flow is neglected. Hence, only two regions form (a mushy and full liquid region) the eutectic reaction is avoided and macrosegregation is not modeled. Fang *et al.* [15] present a similar study that includes three phases, solid, mush and liquid. In this work, however, conditions are such that a eutectic phase does not form and fluid flow leading to macrosegregation is neglected. Worster [16] presents a more complete similarity solution for an aqueous solidification system. This solution includes three phases and a eutectic reaction but still does not account for fluid flow or macrosegregation. This feature is addressed in later work by Chiareli and Worster [4] who include fluid flow and macrosegregation. The model in this case, however, does not include a solid phase or a eutectic reaction.

The objective in this paper is to develop a similarity solution for the system shown in Fig. 1. This solution is applied to a system that has many features that distinguish it from previous similarity solution systems:

(1) The system includes fluid flow and macrosegregation along with a eutectic reaction and a fully solid phase.
(2) The alloy under consideration is more general in nature. In particular it can exhibit finite solubility and can have a finite diffusion of solute in the solid phase, i.e. the value of β and k in equation (4) can be non zero.
(3) With appropriate interpretation and simplifications of the phase diagram the solution can be applied to multicomponent alloys, e.g. a ternary alloy.

4. THE SIMILARITY SOLUTION

In keeping with earlier similarity solutions the appropriate similarity variable is

$$\xi = \frac{z}{2\sqrt{\kappa t}}. \tag{11}$$

The movements of the eutectic and liquidus fronts are assumed to follow the relationships

$$Z_{\text{liq}} = 2\lambda\sqrt{\kappa t}, \quad Z_{\text{eut}} = 2\mu\sqrt{\kappa t} \tag{12}$$

such that in the ξ space these fronts are fixed at $\xi = \lambda$ and $\xi = \mu$, respectively. On defining a velocity term

$$U^* = \sqrt{\frac{t}{\kappa}}U \tag{13}$$

the governing partial differential equations, equations (2)–(6), can be reduced to a set of ordinary differential equations in terms of similarity variable, ξ.

In the liquid region : $\xi \geqslant \lambda$.

Heat

$$2\xi\frac{dT}{d\xi} = \frac{d^2T}{d\xi^2}. \tag{14}$$

In the mushy region : $\mu \leqslant \xi \leqslant \lambda$.

Heat

$$\frac{d^2T}{d\xi^2} = -2\xi[(1-\phi)+\phi R]\frac{dT}{d\xi}+2U^*\frac{dT}{d\xi}+2R\xi\frac{L}{c}\frac{d\phi}{d\xi}. \tag{15}$$

Concentration

$$\frac{d\phi}{d\xi} = \frac{\xi[(1-\phi)+\beta k\phi R]-U^*}{(1-k)RT\xi}\frac{dT}{d\xi} \tag{16}$$

where the liquidus line, equation (1), has been used to eliminate the liquid concentration, C_l, in favor of the temperature T. If required the volume averaged concentration in the solid at each point in the mushy region can be calculated on solving the differential equation

$$\frac{d\phi < C_s >^s}{d\xi} = -T\frac{k}{m}\frac{d\phi}{d\varepsilon}-\beta\phi\frac{k}{m}\frac{dT}{d\xi} \tag{17}$$

where $\langle C_s\rangle^s$ is the intrinsic volume average and once again equation (1) has been used to eliminate the liquid concentration.

Mass

$$\frac{dU^*}{d\xi} = (R-1)\xi\frac{d\phi}{d\xi}. \tag{18}$$

In the solid region : $0 \leqslant \xi \leqslant \mu$.

Heat

$$2\xi\frac{dT}{d\xi} = R\frac{d^2T}{d\xi^2}. \tag{19}$$

In the similarity variable the boundary conditions become

As $\xi \to \infty$

$$T \to T_L + T_{SH}. \tag{20}$$

On the boundary $\xi = \lambda$

$$T = T_L, \quad \left[\frac{dT}{d\xi}\right] = 0, \quad \phi = 0. \tag{21}$$

On the boundary $\xi = \mu$

$$T = T_{eut}, \quad \left[\frac{dT}{d\xi}\right] = -2R(1-\phi)\mu\frac{L}{c},$$
$$[U^*] = \mu(1-R)(1-\phi). \tag{22}$$

At $\xi = 0$

$$T = T_{chill}. \tag{23}$$

In the fully solid and fully liquid regions analytical solutions for the temperature can be obtained

$$T = (T_L+T_{SH}) - \frac{T_{SH}}{\text{erfc}(\lambda)}\text{erfc}(\xi) \tag{24}$$

and

$$T = T_{chill} + \frac{T_{eut}-T_{chill}}{\text{erf}(\mu\sqrt{R})}\text{erf}(\xi\sqrt{R}) \tag{25}$$

respectively. From these solutions the temperature gradients on the liquid side and solid side of the mushy region can be found, i.e. at $\xi = \lambda^+$

$$\frac{dT}{d\xi} = \frac{2}{\sqrt{\pi}}\frac{T_{SH}}{\text{erfc}(\lambda)}e^{-\lambda^2} \tag{26}$$

and at $\xi = \mu^-$

$$\frac{dT}{d\xi} = \frac{2}{\sqrt{\pi}}\frac{\sqrt{R}(T_{eut}-T_{chill})}{\text{erf}(\mu\sqrt{R})}e^{-(\mu\sqrt{R})^2}. \tag{27}$$

In the mushy region the similarity equations, equations (15)–(18), have to be solved numerically. Adopting and extending the approach of Chiareli and Worster [4] a nested shooting method with an Euler solution is employed. The mushy region, $\mu \leqslant \xi \leqslant \lambda$, is discretised into 4000 divisions. Then the following iterative steps are employed :

(1) Values for λ, μ and $U^*|_{\varepsilon=\lambda}$ are guessed.
(2) For the current choices of λ and μ the integration size is evaluated.
(3) Using the condition of continuity of temperature gradient at $\xi = \lambda$, equation (21) and the expression in equation (26) the temperature gradient on the mushy side of $\xi = \lambda$ is evaluated.
(4) Starting at $\xi = \lambda$ and stepping down to $\xi = \mu$ the mushy equations, equations (15)–(18) are solved as initial value problems using an Euler solver.
(5) Based on closing the difference between the calculated temperature at $\xi = \mu$ and the given value, T_{eut}, the value of λ is updated. Following each update steps 2–4 are repeated. This continues until convergence.
(6) Following step 5 the temperature gradient on the solid side of $\xi = \mu$ is evaluated with equation (27). Then on using the jump condition in the temperature gradient at $\xi = \mu$, equation (22), the value of μ is updated.
(7) If convergence at step 6 is not achieved, the calculated temperature gradient on the mushy side

Table 1. Properties and conditions used in test problems

Property	Value	Unit
c	1000	$\mathrm{J\,kg^{-1}\,K^{-1}}$
K	100	$\mathrm{W\,m^{-1}\,K^{-1}}$
L	4×10^5	$\mathrm{J\,kg^{-1}}$
T^*_{eut}	821.2	K
T^*_{F}	921.2	K
T^*_{L}	904.2	K
T^*_{chill}	621.2	K
ΔT_{SH}	1.0	K
k	0.15	—
ρ_{l}	2400	$\mathrm{kg\,m^{-3}}$
ρ_{s}	3120	$\mathrm{kg\,m^{-3}}$
C_0	5.0	wt.%
m	3.4	—

*Note in the similarity solution these temperatures are scaled such that $T^*_{\mathrm{F}} = 0$

of $\xi = \mu$ and the gradient evaluated from equation (27) fail to satisfy the jump condition in equation (22), steps 2–6 are repeated.

(8) On convergence at step 7 the calculated value of the interdendritic flow, U^*, at $\xi = \mu$ is compared with the target value, equation (22). The difference between the calculated and target value is used as a mechanism to update the flow at $\xi = \lambda$.

(9) If convergence at step 8 is not achieved steps 2–8 are repeated.

(10) Convergence at step 9 provides the complete solution.

(11) Following complete convergence the mixture concentration at each point (integration step i) in the mushy region is calculated as

$$[C]_i = \frac{\rho_{\mathrm{s}}(\phi < C_{\mathrm{s}} >^{\mathrm{s}})_i - \rho_{\mathrm{l}}(1-\phi_i)\dfrac{T_i}{m}}{\rho_{\mathrm{l}}\phi_i + \rho_{\mathrm{s}}(1-\phi_i)}. \qquad (28)$$

In this routine some of the correction steps required underrelaxation, with appropriate choices; however, a complete convergence can be obtained in a matter of seconds on a personal computer. The choice of 4000 steps in the mushy region may seem excessive but it is required for accurate solutions independent of the step size. The amount of steps required is a result of using a first-order Euler scheme the application of a fourth-order Runge–Kutta scheme would require fewer steps.

5. TESTING

5.1. *Basic testing*

Testing is carried out with a test alloy with properties consistent with an Al–Cu alloy. The difference between the solid and liquid densities has been enhanced however to fully test the similarity solutions handling of fluid flow and macrosegregation. The appropriate test data, boundary conditions and geometric data (corresponding to the mold arrangement in Fig. 1) is given in Table 1.

In the first instance the similarity solution is used to predict the level of macrosegregation across the mushy region, $\mu \leqslant \xi \leqslant \lambda$, in the case of complete diffusion of the solute at the local scale, $\beta = 1$ in equation (4). Figure 3 plots the macrosegregation profile in terms of the similarity variable. As a point of comparison predictions obtained at three different time steps with a full numerical model [2] are collapsed on to this curve. The comparison is excellent indicating a sound consistency between a complete numerical solution of the governing partial equations and the similarity solution based on the transformed ordinary differential equations. The very small differences can be attributed to grid errors in the numerical model and to the use of the first order Euler solver in the similarity solution. Figure 4 shows similar results to those in Fig. 3. In this case, however, the microsegregation parameter in equation (4) is $\beta = 0$, corresponding to the Scheil assumption of no solid state mass diffusion of solute. Once again the comparison with numerical predictions is excellent, confirming that the proposed similarity solution can effectively deal with the full range of microsegregation behavior. In order that other researchers can readily use the similarity solution to check the performance of proposed numerical schemes the values of the concentrations across the mushy region presented in Figs. 3 and 4 are tabulated in Table 2.

5.2. *Extensions*

In limited cases the proposed similarity solution can be applied to a multicomponent system. The restriction is that the microsegregation parameter, β, and the partition coefficient, k, are constant for each solute species. In this case, due to the condition of mass continuity, the ratio between the concentrations in the liquid phase will remain constant, e.g. for a ternary alloy with two solute components (A and B)

$$C_{\mathrm{A}} = \alpha\frac{m_{\mathrm{B}}}{m_{\mathrm{A}}}C_{\mathrm{B}} \qquad (29)$$

where α is a fixed ratio. Using this expression in the phase diagram leads to explicit relationships between the species concentrations and the temperature, i.e.

$$C_{\mathrm{A}} = -\frac{\alpha T}{(\alpha+1)m_{\mathrm{A}}}, \quad C_{\mathrm{B}} = -\frac{T}{(\alpha+1)m_{\mathrm{B}}}. \qquad (30)$$

In this way, on summing the individual concentration equations for each species, the similarity equations in the mushy region are identical to those used with the binary alloy. Although limited it is noted that this multicomponent solution is an excellent test problem for general purpose solidification codes, see the example in the companion paper [2].

5.3. *Limitations*

In terms of modeling realistic macrosegregation problems there are two limitations with the current similarity solution.

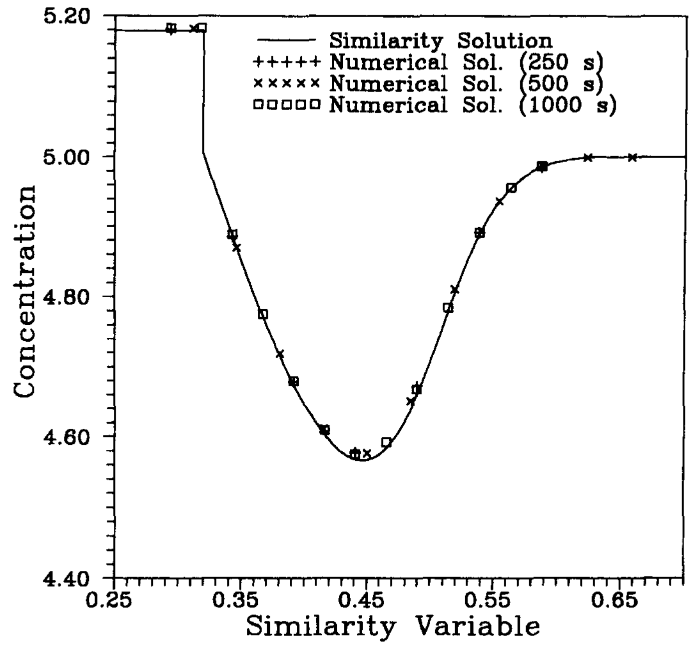

Fig. 3. Concentration profile for lever rule.

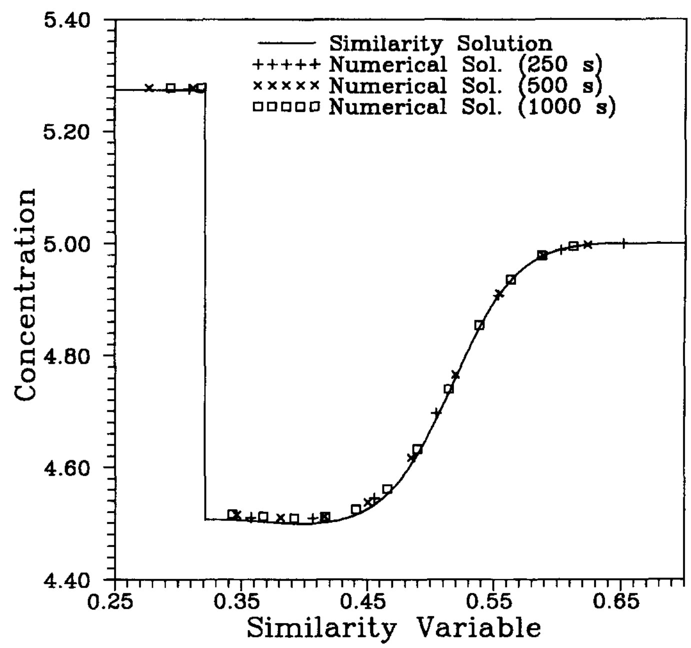

Fig. 4. Concentration profile for Scheil assumption.

(1) Due to the assumption of negligible heat advection in the full liquid the similarity solution may be limited to problems with a low superheat. Numerical experimentations, however, shows that the accuracy of the solution is not greatly effected by the treatment of the full liquid region. Figure 5 shows the mushy region macrosegregation similarity profile ($\beta = 0$) when $\Delta T_{SH} = 25$ as opposed to $\Delta T_{SH} = 1$. Comparison with the profile predicted by a complete numerical solution, a solution that includes a full treatment of the liquid phase, indicates that the loss in accuracy in the similarity solution with this high superheat is very small.

(2) In the similarity solution a fixed constant chill temperature, T_{chill}, is used. This condition forces a constant level of macrosegregation in the full solid region. A condition that is required if a similarity solution across the mushy region is to be obtained. By definition of the similarity solution all the conditions on the eutectic and liquidus fronts have to remain constant in time. In a real

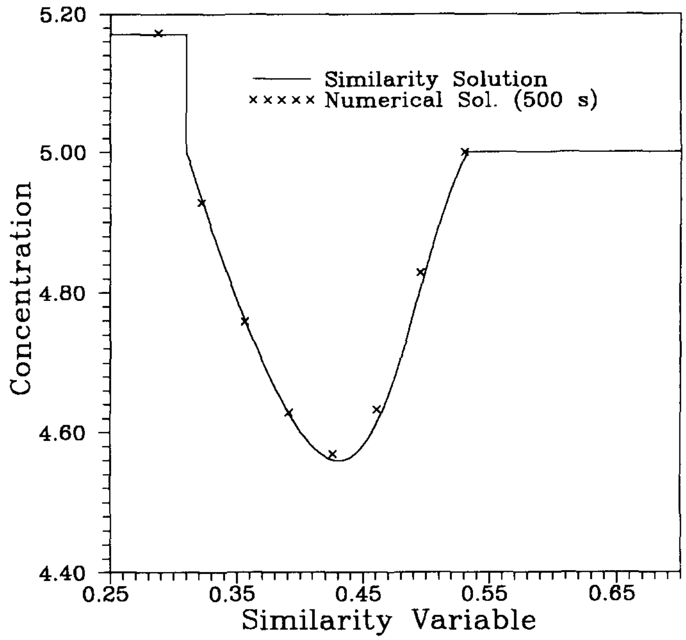

Fig. 5. Concentration profile for lever rule when $\Delta T_{SH} = 25$.

Table 2. Concentration values in mushy region

Lever model $\beta = 1$		Scheil model $\beta = 0$	
Similarity variable ξ	Concentration C	Similarity variable ξ	Concentration C
0.319834 (μ^-)	5.17910	0.321057 (μ^-)	5.27403
0.319834 (μ^+)	5.00644	0.321057 (μ^+)	4.50680
0.350665	4.84868	0.352720	4.50480
0.381495	4.71386	0.384348	5.50041
0.412325	4.61331	0.416048	4.50133
0.443155	4.56732	0.447711	4.52210
0.473986	4.60417	0.479375	4.58732
0.504816	4.73062	0.511038	4.71647
0.535646	4.87633	0.542702	4.86656
0.566477	4.96078	0.574365	4.95792
0.597307	4.99134	0.606029	4.99096
0.628137 (λ)	5.00000	0.637692 (λ)	5.00000

system, based on the geometry in Fig. 1, the chill temperature will change with time, a convective cooling condition is typical. In such cases a so called inverse segregation profile is established in the full solid [17]. This profile takes a large value at the chill face and decreases away from the chill. Predicting a typical inverse segregation profile is beyond the reach of the current similarity solution.

6. CONCLUSIONS

A semi-analytical similarity solution for the solidification of an alloy has been proposed. The solution offers computational advantages over a full numerical solutions of the set of governing partial differential equations in that it only requires the numerical solution of a set of ordinary differential equations. The numerical methods employed to solve these equations are very standard and robust and as a result there is a high degree of confidence that the similarity solution is an accurate solution of the given solidification model.

The solution presented in this paper has features not found in previous similarity solutions [2, 14–16]. In particular

(1) The solution can be applied to problems that have finite partition coefficients and involve finite levels of local solute diffusion in the solid state.
(2) The solution can model problems with fluid flow, macrosegregation and eutectic reactions.
(3) In limited cases a similarity solution for the solidification of a multicomponent alloy systems can be obtained.

Results from the similarity solution have been shown to be fully consistent with results obtained by a complete numerical solution of the governing partial differential equations. This confirms that the proposed similarity solution is an excellent means for testing proposed numerical solutions of alloy solidification problems.

Acknowledgements—The author acknowledges the support of the Minnesota SuperComputer Institute.

REFERENCES

1. Crank, J., *Free and Moving Boundary Problems*. Clarendon Press, Oxford, 1984.
2. Swaminathan, C. R. and Voller, V. R., Towards a general numerical scheme for solidification systems. *International Journal of Heat and Mass Transfer*, 1997, **40,** 2859–2868.
3. Clyne, T. W. and Kurz, W., Solute redistribution during solidification with rapid state diffusion. *Metallurgical Transactions A*, 1981, **12,** 965–971.
4. Chiareli, A. O. P. and Worster, M. G., On measurement and prediction of the solid fraction within mushy layers. *Journal of Crystal Growth*, 1992, **125,** 487–494.
5. Goodman, T. R., The heat balance integral and its application to problems involving a change of phase. *Transactions of ASME*, 1958, **80,** 335–342.
6. Tien, R. H. and Geiger, G. E., A heat-transfer analysis of the solidification of a binary eutectic system. *Journal of Heat Transfer*, 1967, **89,** 230–234.
7. Tien, R. H. and Geiger, G. E., The uni-dimensional solidification of a binary eutectic system with a time-dependent surface temperature. *Journal of Heat Transfer*, 1968, **90,** 27–31.
8. Cho, S. H. and Sunderland, J. E., Heat-conduction problems with melting or freezing. *Journal of Heat Transfer*, 1969, **91,** 421–426.
9. Muehlbauer, J. C., Hatcher, J. D., Lyons, D. W. and Sunderland, J. E., Transient heat transfer analysis of alloy solidification. *Journal of Heat Transfer*, 1973, **95,** 324–331.
10. Voller, V. R., Development and application of a heat balance integral method for analysis of metallurgical solidification. *Applied Mathematics Modeling*, 1989, **13,** 3–11.
11. Flemings, M. C. and Nero, G. E., macro-segregation, part 1. *Transactions of the Metallurgical Society AIME*, 1968, **242,** 41–49.
12. Rubinstein, Li, The Stefan problem. *Transactions of Mathematical Monographs*, Vol. 27. American Mathematical Societies, 1971.
13. Goodman, T. R., Discussion of a heat-transfer analysis of the solidification of a binary eutectic system. *Journal of Heat Transfer*, 1967, **89,** 230–234.
14. Braga, S. L. and Viskanta, R., Solidification of a binary solution on a cold isothermal surface. *International Journal of Heat and Mass Transfer*, 1990, **33,** 745–754.
15. Fang, L. J., Cheung, F. B., Linehan, J. H. and Pedersen, D. R., Selective freezing of a dilute salt solution on a cold ice surface. *Journal of Heat Transfer*, 1984, **106,** 385–393.
16. Grae Worster, M., Solidification of an alloy cooled from a boundary. *Journal of Fluid Mechanics*, 1986, **167,** 481–501.
17. Voller, V. R. and Sundarraj, S., A model of inverse segregation: the role of microporosity. *International Journal of Heat and Mass Transfer*, 1995, **38,** 1009–1018.